CONTRAST MEDIA & MOLECULAR IMAGING

Received: 9 September 2015, Revised: 7 March 2016, Accepted: 20 March 2016, Published online in Wiley Online Library: 15 June 2016

(wileyonlinelibrary.com) DOI: 10.1002/cmmi.1697

The effect of superparamagnetic iron oxide nanoparticles surface engineering on relaxivity of magnetoliposome

Sepideh Khaleghi[a], Fatemeh Rahbarizadeh[a]*, Davoud Ahmadvand[b], Mahrooz Malek[c] and Hamid Reza Madaah Hosseini[d]

The purpose of this work is evaluating the effect of ultra small superparamagnetic iron oxide nanoparticles (USPIONs) coatings on encapsulation efficiency in liposomes and cellular cytotoxicity assay. Moreover, we assessed the effects of surface engineering on the relaxivity of magnetoliposome nanoparticles in order to create a targeted reagent for the intelligent diagnosis of cancers by MRI. For estimating the effect of nanoparticle coatings on encapsulation, several kinds of USPIONs coated by dextran, PEG5000 and citrate were used. All kinds of samples are monodispersed and below 100 ± 10 nm and the coatings of USPIONs have no significant effect on magnetoliposome diameter. The coating of USPIONs could have effect on percentage of encapsulation. The dextran coated USPIONs have more stability and quality accordingly the encapsulation increased up to 92%, then the magnetoliposome nano particles have been targeted by Herceptin and anti-HER2 VHH, separately. Over storage period of four weeks the resulting particles were stable and physico-chemical properties such as size and zetapotential did not show any significant changes. The relaxivity of contrast agents was measured using a 1.5 T MRI. The r2/r1 ratio was more than two for all samples which demonstrate the negative contrast enhancing of all SPION embedded specimens. The high ratio of r2/r1 as well as high r2 is the best combination of a negative contrast agent as it is obtained for pure magnetite. The value of r2/r1 for all other samples including Herceptin targeted magnetoliposome, anti-HER2 VHH targeted magnetoliposome and non-targeted magnetoliposome were between ~21 to ~28, which show the magnetite embedded samples have enough negative contrast to be detectable by MRI. Therefore the HER2 targeted magnetoliposomes are a good and stable candidate as contrast agents in clinical radiology and biomedical research with minimal cytotoxicity and biocompatibility effects. Copyright © 2016 John Wiley & Sons, Ltd.

Keywords: magnetoliposome; surface engineering; relaxivity, cytotoxicity

1. INTRODUCTION

Thanks to its improved resolution and unlimited tissue penetration, magnetic resonance imaging (MRI) is one of the most efficient diagnostic modalities in clinical radiology and biomedical research today (1). MRI ranks among the best noninvasive methodologies today available in clinical medicine for assessing anatomy and function of tissues. Its main advantages are that it allows rapid *in vivo* acquisition of images and, under specific conditions, it makes possible imaging at cell resolution (2,3). In order to improve contrast images, the use of exogenous substances or contrast agents that alter signal intensity by selectively shortening the hydrogen relaxation times of the tissues becomes essential to improve sensitivity and specificity of MRI. The use of contrast agents such as paramagnetic Gd^{3+} (referred to as a positive, *T*1-contrast agent) or super paramagnetic iron oxide nanocores (a so-called negative, T2-contrast agent) is a common practice to enhance detection limits and visualization of targeted organs or cells (4). The most commonly used magnetic nanoparticles (MNPs) are composed of an iron oxide core consisting of crystal magnetite (Fe_3O_4) or maghemite (γFe_2O_3) (5,6). Because of high toxicity of Gd^{3+}, for *in vitro* cell labeling experiments or long-term *in vivo* cell tracking studies, the clearance of the particles should be slight. Iron oxide nanoparticles may potentially provide higher contrast enhancement in MRI than conventional Gd complexes contrast agents because of their super paramagnetic property. For this reason ultra small super paramagnetic iron oxide nanoparticles (USPIONs) are most favorable (7,8).

* *Correspondence to: F. Rahbarizadeh, Department of Medical Biotechnology, Faculty of Medical Sciences, Tarbiat Modares University, P.O. BOX. 14115-331, Tehran, Iran. E-mail: rahbarif@modares.ac.ir*

a *S. Khaleghi, F. Rahbarizadeh*
Department of Medical Biotechnology, Faculty of Medical Sciences, Tarbiat Modares University, P.O. BOX. 14115-331, Tehran, Iran

b *D. Ahmadvand*
School of Allied Medical Sciences, Iran University of Medical Sciences, Tehran, Iran

c *M. Malek*
Department of Radiology, Medical Imaging Center, Advanced Diagnostic and Interventional Radiology Research Center (ADIR), Imam Khomeini Hospital, Tehran University of Medical Sciences (TUMS), Tehran, Iran

d *H. R. Madaah Hosseini*
Materials Science and Engineering Department, Sharif University of Technology, P.O. BOX. 11155-9466, Azadi Avenue, Tehran, Iran

USPIONs coating by dextran, citrate or polyethylene glycol (PEG) and then surface engineering by lipids provides stability and enhanced biocompatibility to these magnetoliposomes nanoparticles (MLs) (9). The bedrock of MLs is basically on the structure and specific features of renowned phospholipid vesicles. Owing to outstanding properties of liposomes such as biocompatibility, wide range of surface manipulations, encapsulation of both hydrophilic (in the inner aqueous cavity) as well as hydrophobic (in the lipid bilayer) compounds, therapeutic and diagnostic applications, liposomes are the most frequently employed carrier vehicles for medical applications (7,9,10). The underlying principle of most current nanotechnology based drug delivery platforms is stood on the enhanced permeability and retention (EPR) effect has proven to be a key pharmacokinetic feature for existing nanomedicines but this mechanism is not applicable to potential nanomedicines that target circulating tumor cells in circulation (11). Active targeting of a nanoparticle is a way to minimize uptake in normal tissue and increase accumulation in a tumor. Strategies for active targeting of tumors usually involve targeting surface membrane proteins that are up regulated in cancer cells (12–15).

One great challenge with active targeted delivery of magnetic nanocarriers is variation in magnetic nanoparticles properties after chemical surface modification. The coating molecules increase water solubility and decrease toxicity and immunogenicity (16). However, the coating may interact with the surface atoms of the magnetic core to form a nonmagnetic layer, reducing its effective size and the total amount of magnetic phase, whereas the effective size and especially the concentration of the magnetic phase are important factors in many biomedical applications (17,18).

The majority of researches concerning the effect of nanoparticle coating on cellular uptake, circulatory blood half-life, and the ability to accumulate in tumors is derived from investigations with nonmagnetic nanoparticles, whereas information concerning the effect of MNP coatings and targeting on relaxometry are still rare. In some studies the decrease was attributed to the surface chemical interaction between the stabilizing surfactant and the magnetic core. Recently, Vestal and Zhang showed that the coercivity and saturation magnetization of manganese ferrite nanoparticle change after surface modification with para-substituted benzoic acid ligands and substituted benzene ligands (17,19). Only a few studies have been reported on the reduction of the magnetic phase in coated nanoparticle systems (20), and none have focused on the changes made by the surface engineering and antibody targeting. Actually different kinds of targeting agents such as monoclonal antibodies (mAbs) (13) and peptides may have detrimental effects on biocompatibility and relaxometry. In this study we decide to utilize Herceptin (a mAb against HER2) and anti-HER2 VHH (a small molecule as a small ligand). Herceptin interferes with the HER2/neu receptor (the second member of the EGFR (ErbB) family) and since gene amplification and/or over-expression of HER2 occur in 20–30% of breast cancers, it makes it an attractive target for intelligent theranostics. Furthermore VHHs are the next generation of therapeutic agents that ideally encompass the advantages of small molecules as well as the benefits of mAbs. VHHs are smallest available intact antigen-binding units in comparison with mAbs, derived from functional heavy-chain antibodies (HCAbs) devoid of light chains (21). In current work, we address the effects of different kinds of magnetite coatings (dextran, PEG5000 and citrate coated USPIONs) on encapsulation efficiency and cytotoxicity then the effect of targeting will be investigated by anti-HER2 VHH and whole Herceptin antibody on the relaxivity of magnetoliposomes.

2. MATERIALS AND METHODS

2.1. Chemicals and reagents

1,2-dipalmitoyl-sn-glycero-3-phosphocholine (DPPC), cholesterol, 1,2-distearoyl-sn-glycero-3-phosphoethanolamine-N-[methoxy(polyethylene glycol)-2000] (ammonium salt) (DSPE-mPEG(2000)) and 1,2-distearoyl-sn-glycero-3-phosphoethanolamine-N-[maleimide (polyethylene glycol)-2000] (ammonium salt) (DSPE-PEG(2000) maleimide) were purchased from Avanti polar lipids. USPIONs coated by dextran and PEG5000 provided in (Biomaterial laboratory, Sharif University of Technology, Tehran, Iran) (22) and USPIONs coated by citrate were bought from Institute of Teb Sanat Rahyab (Tehran, Iran). 3-(4, 5-Dimethylthiazol-2-yl)-2, 5-diphenyltetrazolium bromide (MTT) salt was bought from Sigma-Aldrich (St. Louis, MO, USA). The Quick Start™ Bradford protein assay kit provided from Bio-Rad Laboratories Inc. PrestoBlue™ Cell Viability reagent was obtained from Life technology (Carlsbad, CA, USA). Plastic disposable 96-well tissue culture dishes, pipettes and tubes were purchased from Nunc (Roskilde, Denmark).

2.2. Cell culture conditions

BT-474 (HER2-overexpressing breast cancer cell line) and MDA-MB-231 (HER2 and estrogen receptor negative breast cancer cell line) were grown in RMPI (100 U/mL penicillin, 100 μg/mL streptomycin and 2 mM/L glutamine) with or without 10% FBS and SK-BR-3, MCF-10A (human normal breast epithelial cell line) was cultured in the DMEM/F12 medium supplemented with 5% horse serum, 100 mg/mL EGF, 1 mg/mL hydrocortisone, 10 mg/mL insulin, 100 units/mL of penicillin and 100 μg/mL of streptomycin.

2.3. Preparation of magnetoliposomes

The magnetoliposomes were prepared using the classical film rehydration method followed by extrusion according with the work of Sabate *et al*. (2008) with some modifications (23). In brief, the lipids DPPC: cholesterol: DSPE-PEG2000: malemide-PEG2000-DSPE in a molar ratio of 7:2.5:0.4:0.1 and in amounts required to obtain a final lipid concentration of 50 mg/mL, were dissolved in a mixture of chloroform and methanol (9:1, volume ratio) in a round-bottom flask and dried in a rotary evaporator under reduced pressure at 45 °C to form a thin film on the flask. After the complete removal of the chloroform, the lipid film was hydrated with the appropriate amount of the mixture of water and USPIONs to give a lipid concentration of 50 mg/mL for 1 h. Multilamellar liposomes (MLV) were downsized to form oligolamellar vesicles by mini-extruder (Avanti Polar Lipids, AL, USA) with polycarbonate membranes (Avanti Polar Lipids) with pore diameters of 100 nm 21 times at 45 °C.

2.4. Particle characterization

2.4.1. Size and electro kinetic determination

In ferrofluid and magnetoliposomes, the mean and distribution of the particle size were determined by dynamic light scattering at 25 °C with a Zetasizer Nano ZS90 (Malvern, UK). To measure

particle size distribution of the dispersion, a polydispersity index (PDI), ranging from 0.0 for an entirely monodisperse sample to 1.0 for a polydisperse sample, was used. Electrophoretic mobility was measured with a Zetasizer Nano ZS90 (Malvern, UK) too. Magnetoliposomes were diluted with PBS 10 mM until a concentration of approximately 0.2 g/L of magnetite. To avoid that magnetoliposomes can settle due to the high density of the magnetite, the measurement was carried out with three different samples.

2.4.2. Transmission electron microscopy

The final magnetoliposomes were detected by transmission electron microscopy (TEM) using a Hitachi H-7500 transmission electron microscope. Sample was arranged by placing a drop of magnetoliposomes onto a 400-mesh copper grid coated with carbon film, and it was tolerated to dry in the air before introduction into the microscope. Scanned images were then analyzed in Adobe® ImageReady™, version 3.0, to determine approximate diameters.

2.5. Purification of magnetoliposomes

After the process of sample sizing, non-entrapped ferrofluid particles were removed by size exclusion chromatography (SEC) with a 1×30 cm chromatography column (sepharose CL4B, Sigma-Aldrich, St. Louis, MO, USA) saturated with lipids before sample elution. The elution profiles of liposomes and IONPs were previously identified to validate the separation procedure in order to obtain the desired iron oxide/lipid ratio for a constant lipid concentration.

2.6. Assay of magnetite

At first, cell pellets are mineralized in a volume of 5 N HCl (100–400 μL depending on the cell number) for 4 h in a water bath at 80 °C or during 24–72 h in a water bath at 37 °C. The standard curve was accomplished by 100 μL of aqueous solutions containing 0.22–2.2 μg Fe of the USPION suspension (~39–390 μM Fe), or 0.625–2.5 μg Fe of ferric iron solution (~112–448 μM Fe) were treated over 24 h at 37 °C with 100 μL 5 N HCl, it follows that the solution was mixed with 100 μL of 5% Potassium Ferrocyanide, Perl's reagent, in distilled water. The absorbance of the solution was read at 630 nm or 650 nm after 15 min.

2.7. Assay of phospholipids

Phospholipid content in magnetoliposomes was determined by the method of Steward-Marshall (1980) and phosphate assay kit (Colorimetric) (Abcam, Cambridge, USA). It was confirmed in advance that the presence of ferritine had no influence on color development. An aliquot of 50 μL of magnetoliposomes was mixed with 500 μL of $CHCl_3$, before adding 500 μL of the reagent (0.1 M ammonium ferrothiocyanate). After shaking energetically for 45 s, the sample was centrifuged for 10 min at 2000 rpm. The absorbance of the aqueous phase was read at 490 nm. The calibration curve was performed with several amounts of a 40 mM solution of phosphatydylcholine in $CHCl_3$.

2.8. Encapsulation efficiency determination

For establishment the best magnetite/phospholipid ratio, liposomes containing 5–45 mg of magnetite per mol of phospholipids were prepared. After SEC purification, the amount of magnetite and the phospholipid content were determined, the magnetite/phospholipid ratio was calculated, and this value was compared to the initial pre-SEC values to obtain the percentage of encapsulation. In order to evaluate the effect of nanoparticle coatings on encapsulation, several kinds of USPIONs coated by dextran, PEG_{5000} and citrate were used.

2.9. Cell viability and metabolic activity

2.9.1. MTT assay

To evaluate the effect of nanoparticles on the viability of the cells, a 3-(4,5-Dimethylthiazol-2-yl)-2,5-diphenyltetrazolium bromide (MTT) assay was established. For this purpose BT-474, SK-BR-3, MCF10-A and MDA-MB-231 cell lines were seeded on 96-well microtiter plate at a density of 4×10^4, 3×10^4, 2×10^4 and 3×10^4 respectively, then incubated with magnetoliposomes (200 and 400 μg Fe/ml), liposomes (adjust to magnetoliposomes) and magnetites coated by dextran, PEG_{5000} and citrate (200 and 400 μg Fe/ml) for 24 and 48 h. After incubation, all samples were washed three times with PBS (without Mg^{2+} and Ca^{2+}) and further incubated for 4 hours at 37 °C and 5% CO2 with MTT solution (0.5 g/L in medium) and phenol red free medium according to data sheet until purple precipitate is visible. The medium was then removed and 100 μL lysis buffers (1% Triton X-100 in isopropanol) were added to each well and extensively mixed. The optical density was then measured at 570 nm using a Nunc absorbance plate reader (Roskilde, Denmark). The viability of cells was represented as percent of viability normalized to non-labeled samples (100%).

2.9.2. CytoTox 96® cell membrane permeability assay

In order to overcome any of the nano particle-associated problems, it is important to add control samples and preferably to use different assays which are based on different cellular parameters. The CytoTox 96® assay quantitatively measures lactate dehydrogenase (LDH), a stable cytosolic enzyme that is released upon cell lysis. Released LDH in culture supernatants is measured with a 30 min coupled enzymatic assay, which

Table 1. Characteristics of the obtained PEGylated magnetoliposomes with several concentrations of Citrate coated USPIONs. ML1, ML2 … ML7 are magnetoliposome samples with several amounts of magnetite/mol of phospholipid (5–45 g Fe3O4/mol PL)

Citrate coated USPIONs	ML1	ML2	ML3	ML4	ML5	ML6	ML7
gFe3O4/mol PL	5	10	15	20	25	35	45
gFe/mol PL	3.6	7.1	10.7	14.3	17.8	25.0	32.1
% encapsulation	7 ± 0.5	8.5 ± 0.1	9 ± 0.1	9.5 ± 0.1	10 ± 0.8	9 ± 0.1	8 ± 0.2
Z-average hydrodynamic diameter (nm)	105	109	110.5	109.5	112	111	112
polydispersity index (PDI)	0.1	0.1	0.1	0.1	0.1	0.1	0.1

Table 2. Characteristics of the obtained PEGylated magnetoliposomes with several concentrations of PEG coated USPIONs. ML1, ML2 … ML7 are samples with several amounts of magnetite/mol of phospholipid (5-45 g Fe3O4/mol PL)

PEG coated USPIONs	ML1	ML2	ML3	ML4	ML5	ML6	ML7
gFe3O4/mol PL	5	10	15	20	25	35	45
gFe/mol PL	3.6	7.1	10.7	14.3	17.8	25.0	32.1
% encapsulation	32 ± 0.8	49 ± 0.5	23 ± 0.7	22 ± 0.6	20 ± 0.5	21 ± 0.4	20 ± 0.7
Z-average hydrodynamic diameter (nm)	90	95	98	99	100	102	105
polydispersity index (PDI)	0.1	0.1	0.1	0.1	0.1	0.1	0.1

results in the conversion of a tetrazolium salt (INT) into a red formazan product. The amount of color formed is proportional to the number lysed cells. Because various cell types contain different amounts of LDH, we prepared a preliminary experiment using our target cell populations to determine the optimum number of target cells to use with the CytoTox 96® assay and to ensure an adequate signal-to-noise ratio. The LDH positive control supplied may be used to verify that the LDH assay is functioning properly. After 4 h treatment of the cells with the samples as mentioned above according to manufacture protocol, the viability of cells was represented as percent of viability normalized to non-labeled samples (100%) as mentioned above.

2.9.3. PrestoBlue™ cell viability assay

PrestoBlue™ cell viability reagent is a ready-to-use reagent for rapidly evaluating the viability and proliferation of a wide range of cell types. Presto blue assay was done according to the manufacturer's protocol. After 24 h treatment of the cells with the samples as mentioned above, the cells were washed and incubated with PB reagent. The changes in cell viability were detected using both, fluorescence and absorbance spectroscopy. The absorbance was recorded at 570 nm after 2 h incubation of mentioned cells with PB reagent, whereas the fluorescence was read (excitation 570 nm; emission 610 nm) at recommended time of incubation (20 min and 2 h endpoint). The cell viability was expressed as a percentage relative to the non-treated cells.

2.10. Preparation of anti-HER2 targeted magnetoliposomes

Targeting was done by both Herceptin and anti-HER2 VHH for comparison. In order to conjugate thiolated VHH to liposomes, the buffer was exchanged with phosphate buffer by amicon filter 30000KDa and the pH was adjusted to 7.0. To optimize immunoliposomes preparation, the samples were incubated for 1, 2, 3, and 24 h at 20 °C and 4 °C under constant and gentle shaking. In all samples, 50 mg liposome was added to 1.8 g/L VHH and the volume of the samples was adjusted to 1 mL with phosphate buffer (pH 7). With the purpose of Herceptin conjugation, the antibody thiolated with 50-fold molar excess of 2-iminothiolane for 2 h and the buffer was exchanged as described above, an aliquot (1 g/L) of thiolated Herceptin solution in phosphate buffer pH 7 were added to 50 mg liposome under constant gentle shaking at room temperature for 1 h and the volume of the samples was adjusted to 1 mL with phosphate buffer (pH 7). Conjugation was confirmed by SDS-PAGE followed by silver staining (24).

2.11. Storage stability of anti-HER2 VHH targeted magnetoliposomes

Nanoparticles conjugated with ati-HER2 VHH were prepared and analyzed as described above. Without any additional agents the particle samples were stored in phosphate buffer pH 7 at 4 °C for a period of 4 weeks. Once a week an aliquot (100 μL) of the nanoparticle suspension was analyzed for unbound anti-HER2 VHH using SEC as described above. Additionally, particle size and zetapotential were measured.

2.12. Phantom analysis

The MRI contrast efficiency of the samples was assessed at room temperature by investigating the hydrogen relaxivity (the relaxation rates per iron concentration, expressed in mM). *In vitro* study was performed by 1.5 T GE MR Scanner at 25 °C with a 90 mm × 90 mm field of view (FOV), one acquisition, matrix size of 256 × 196 pixels and 5 mm slice thickness. All sample series were placed in 1.5 mL tubes in a water-filled plastic container to avoid any susceptibility artifact due to air. T_1 and T_2-weighted images with different sample concentrations (0.1, 0.2, 0.4, 0.6, 1 and 1.2 mM Fe/mL) were analyzed quantitatively. The r1 and r2 parameters were calculated by calculating the slope of (1/T1) and (1/T2) plots versus concentrations. T1 weighted Spin-echo images with fixed TE = 12 ms and multiple TR = 240, 500, 1000, 2000 and 4000 ms were applied to calculate R1 in different concentrations. T2 weighted Spin-echo images with fixed

Table 3. Characteristics of the obtained PEGylated magnetoliposomes with several concentrations of Dextran coated USPIONs. ML1, ML2 … ML7 are samples with several amounts of magnetite/mol of phospholipid (5-45 g Fe3O4/mol PL)

Dextran coated USPIONs	ML1	ML2	ML3	ML4	ML5	ML6	ML7
gFe3O4/mol PL	5	10	15	20	25	35	45
gFe/mol PL	3.6	7.1	10.7	14.3	17.8	25.0	32.1
% encapsulation	12 ± 0.1	24 ± 0.7	14 ± 0.2	47 ± 0.1	44 ± 0.5	41 ± 0.6	91 ± 0.9
Z-average hydrodynamic diameter (nm)	100	119	112.5	106.5	112.9	89.0	98.0
polydispersity index (PDI)	0.1	0.1	0.1	0.1	0.1	0.1	0.1

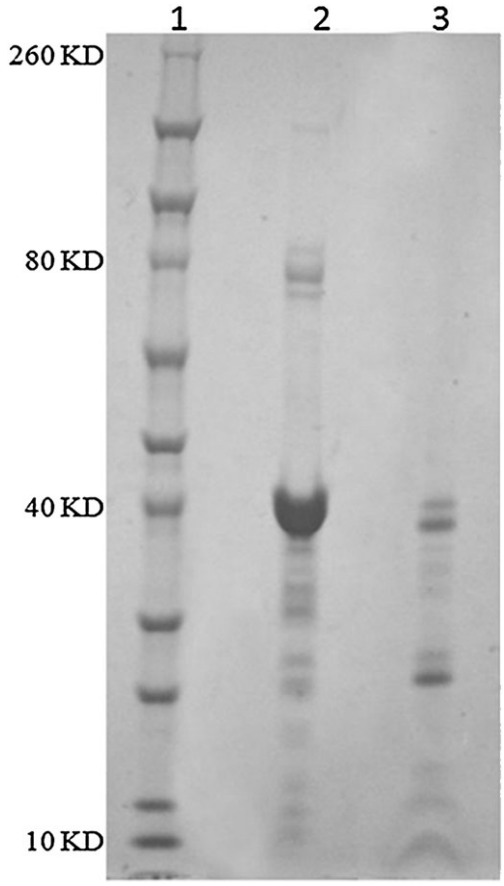

Figure 1. Confirmation of antibody conjugation on the surface of liposomes by coomassie blue staining. The heavier band than VHH to the 3 KD, represent the conjugation of VHH to the surface of magnetoliposomes. 1) protein ladder, 2) purified free VHH and 3) conjugated VHH to ML.

TR = 4000 ms and multiple TE =12, 24, 36 and 48 ms were applied to calculate R2 in different concentrations.

2.13. Statistical analysis

The different experimental groups within the study were compared by using the one way-ANOVA and MANOVA test. The comparisons between the pairs of groups were performed with the Manhane test. A probability of less than 0.05 ($P < 0.05$) was used for statistical significance.

3. RESULTS AND DISCUSSION

3.1. Characterizations of magnetoliposomes

In order to confirm the physical characterization of magnetoliposomes, several usual techniques were used. As-prepared magnetoliposomes (containing 5–45 g of magnetite/mol of phospholipid (Pl)) were brownish appearance and highly soluble in water.

3.1.1. Size and electro kinetic determination

After preparation of magnetoliposomes, the average diameter and distribution of nanoparticles were determined by Zetasizer Nano ZS90 at 25 °C and expressed as z-average. After optimization of encapsulation by serial concentrations of USPIONs, the results show the expected general trend of an increase in the particle diameter with an increase in USPIONs concentration but statistically there's no significant difference among magnetoliposomes with different amounts of Fe_3O_4 in size and z-average (Tables 1–3). All the samples are monodispersed and below 100 ± 10 nm corresponding to the diameter of polycarbonate filter. After surface modification with VHH (Fig. 1) an average size of 110 ± 10 nm with PDI below 0.1 and a surface charge of -5 mV were obtained. Without VHH modification the average size was 100 ± 10 nm and the zetapotential of 0.42 mV near to neutral. However, negative zetapotential after conjugation shows the VHH induces a negative charge on the surface of targeted magnetoliposomes, in order to minimize nonspecific interaction with blood components and off-target cells. The coatings of USPIONs have no significant effect on magnetoliposome diameter and the sizes of the samples are accordance with the poly carbonate filter diameter.

3.1.2. TEM

Figure 2 was obtained by TEM without staining the samples. From these micrographs, we can see that the magnetoliposomes prepared by the improved method of rotary film evaporation and high-pressure extrusion were spherical, with different size, nearly <60 nm predominantly, and most of them were single room. USPION particles were found in a higher extent inside of the liposomes although their distributions were rather irregular. Entrapped USPION particles did not present any specific interaction with the lipid bilayer and they retained good dispersibility.

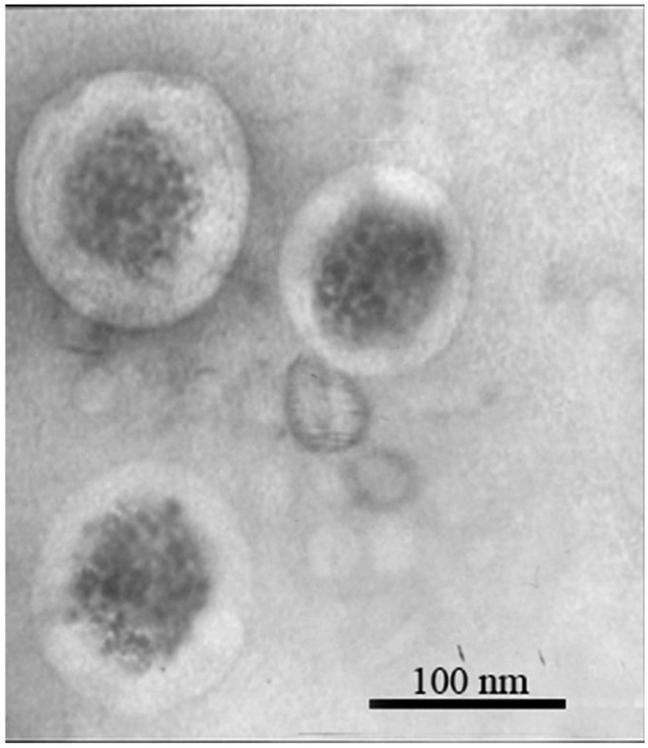

Figure 2. TEM image of MLs without staining, showing the phospholipid bilayer surrounded the electron dense iron oxide cores.

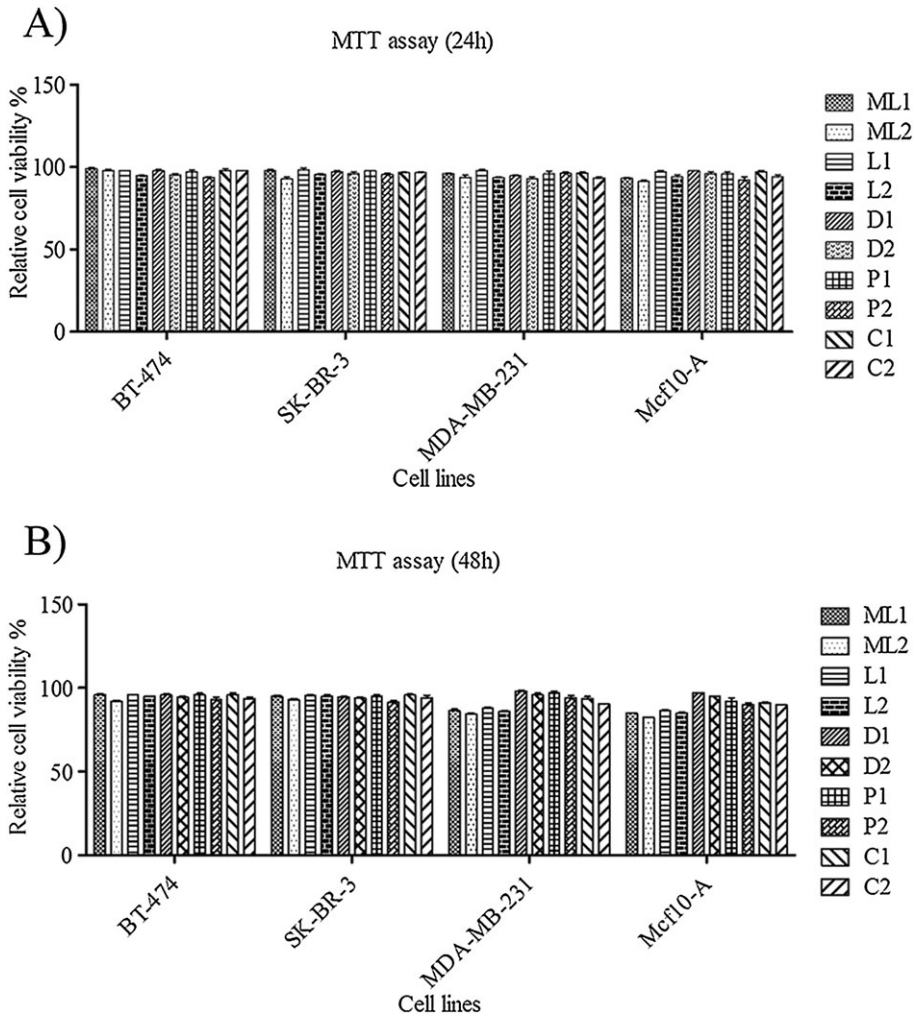

Figure 3. Cell viability assay (MTT) for HER2 positive (SK-BR-3 and BT-474) , HER2 negative (MDA-MB-231) and normal breast cell line (MCF10-A) incubated with magnetoliposome (ML1: 200 μg Fe/mL , ML2: 400 μg Fe/mL), liposome (*L1: liposome 5mgPC/ml, L2: liposome 10mgPC/ml), Dextran coated USPION (*D1: 200 μg Fe/mL, D2: 400 μg Fe/mL), PEG coated USPION (P1: 200 μg Fe/mL, P2: 400 μg Fe/mL) and citrate coated USPION (C1: 200 μg Fe/mL, C2: 400 μg Fe/mL) , after 24 h (A) and 48 h (B) of incubation. The error bars indicated are mean SEM (n ¼ 10). For the cell viability, relative values are given to those of control samples not incubated with any particles but otherwise treated identically.

3.2. Purification and encapsulation efficiency determination

After size exclusion chromatography (SEC) purification by sepharose CL4B, liposomes were recovered completely free of contaminating external ferrofluid in elutes corresponding to the void volume of the column. The encapsulation efficiency was determined with varying initial weight ratios of magnetite to phospholipids, as we wanted to determine the effects of magnetite coatings on encapsulation efficiency, different kinds of coatings; dextran, PEG_{5000} and citrate were determined (Tables 1–3). In all steps, the initial amounts of phospholipids were identical and the synthesis process was the same. Magnetite and phospholipid concentrations were determined before extrusion and after purification by SEC. According to Table 1, the amount of encapsulated iron steadily increases as the starting iron/phospholipid ratio increases from 5 to 45 g Fe_3O_4 /mol Pl. The low percentage of encapsulation at higher concentration ratios can be explained by the loss of magnetite during the extrusion process, since the polycarbonate membrane is completely covered by a dark film of magnetite. Although magnetite is much smaller than the magnetoliposomes, the formation of clusters of ferrofluid particles could explain the presence of magnetite on the surface of membranes (25). The percentage of dextran coated USPIONs encapsulation, which has rapid increase at the lowest initial concentrations (from 5 g Fe_3O_4 /mol Pl to 25 g Fe_3O_4 /mol Pl), remained almost constant (from 25 g Fe_3O_4 /mol Pl to 45 g Fe_3O_4 /mol Pl) and finally decreased (in concentrations greater than 45 g Fe_3O_4 /mol Pl). We obtained the best percent of encapsulation about 92% in 45 g Fe_3O_4 /mol Pl for dextran coated USPIONs, about 50% in 10 g Fe_3O_4 /mol Pl for PEG coated USPIONs and 10% in 25 g Fe_3O_4 /mol Pl for citrate coated USPIONs. Of course the quality and stability of USPIONs coatings has a considerable impact on the encapsulation efficiency. In this experiment the dextran coated USPIONs have more stability and quality accordingly the encapsulation increased. We choose dextran coated USPIONs by 45 g Fe_3O_4 /mol Pl concentration ratios for the best of experimental tests. Consequently, the kind of USPIONs coating could have effect on percentage of encapsulation. This may be due to inappropriate interactions between USPIONs coatings and PEGylated magnetoliposomes.

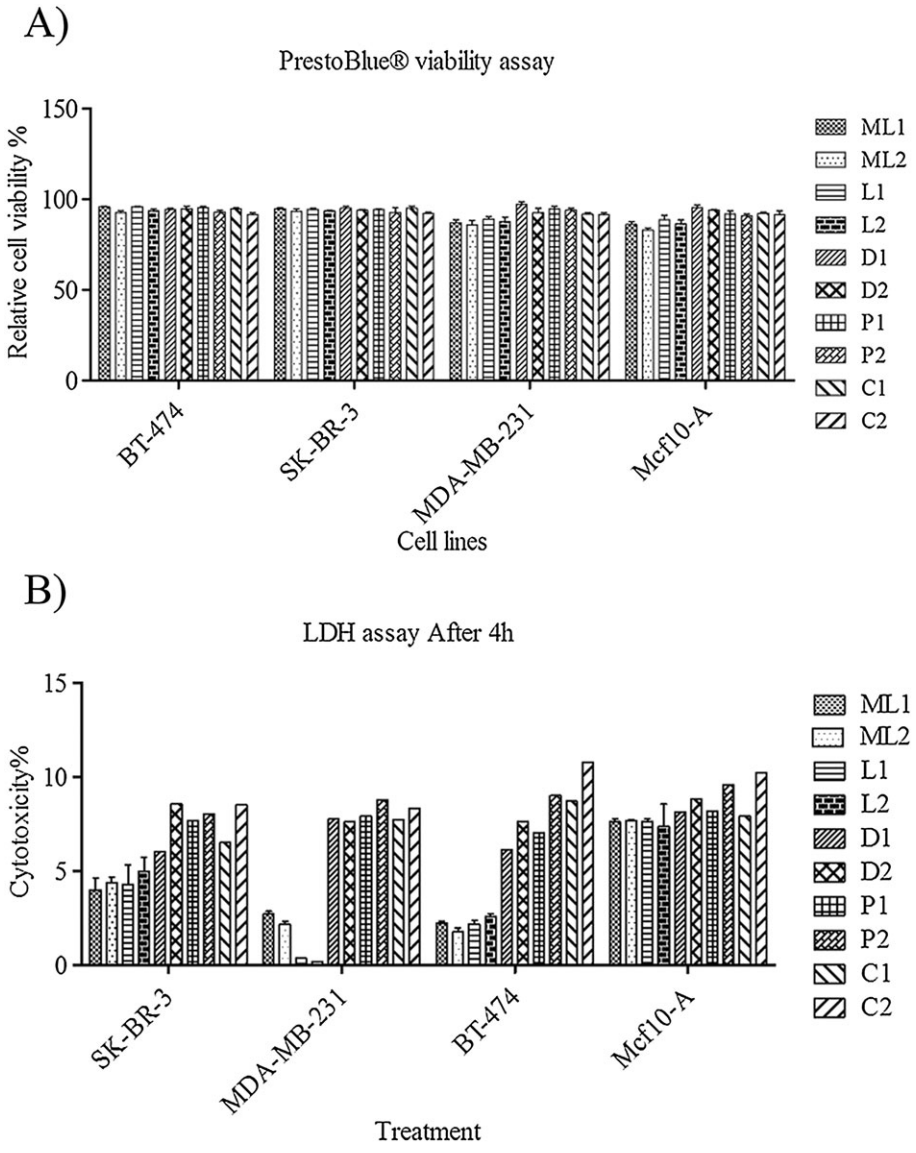

Figure 4. A) CytoTox 96® cell membrane permeability assay. B) PrestoBlue™ cell viability assay. HER2 positive (SK-BR-3 and BT-474) , HER2 negative (MDA-MB-231) and normal breast cell line (MCF10-A) incubated with magnetoliposome (ML1: 200 μg Fe/mL, ML2: 400 μg Fe/mL), liposome (*L1: liposome 5mgPC/mL, L2: liposome 10mgPC/mL), Dextran coated USPION (*D1: 200 μg Fe/mL, D2: 400 μg Fe/mL), PEG coated USPION (P1: 200 μg Fe/mL, P2: 400 μg Fe/mL) and citrate coated USPION (C1: 200 μg Fe/mL, C2: 400 μg Fe/mL), after 4 h and 24 h of incubation for CytoTox 96® cell membrane permeability and PrestoBlue™ cell viability assay respectively. Values for every sample are relative to that of control cells not incubated with MLs or inhibitors.

3.3. Comparison of the cytotoxicity effects of USPIONs coatings, ML and vesicles

To compare the cellular toxicities of dextran, PEG_{5000} and citrate coated USPIONs, MLs and vesicles, we evaluated cell viability in BT-474, SK-BR-3 as HER2 positive breast cancer cell lines, MDA-MB-231 as HER2 negative breast cancer cell lines and MCF10-A as breast normal cell line. These cell lines were incubated with dextran, PEG_{5000} and citrate coated USPIONs, MLs and iron oxide-free vesicles, all containing the same phospholipid ingredients and identical preparation process. All types of particles were given at two different iron concentrations, being 200 and 400 g Fe/L (26–28). These concentrations correspond to the lipid concentration for iron oxide-free vesicles. The viability assay (MTT) after 24 and 48 h (Fig. 3 A, B), LDH assay

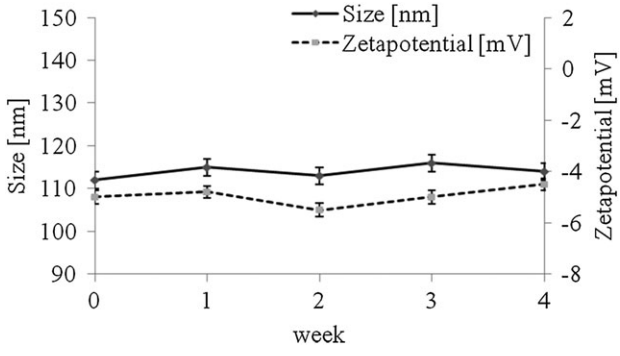

Figure 5. Storage stability of anti-HER2 targeted magnetoliposomes. Particle diameter and zetapotential were recorded over a time period of 4 weeks (n = 3; mean ± SD).

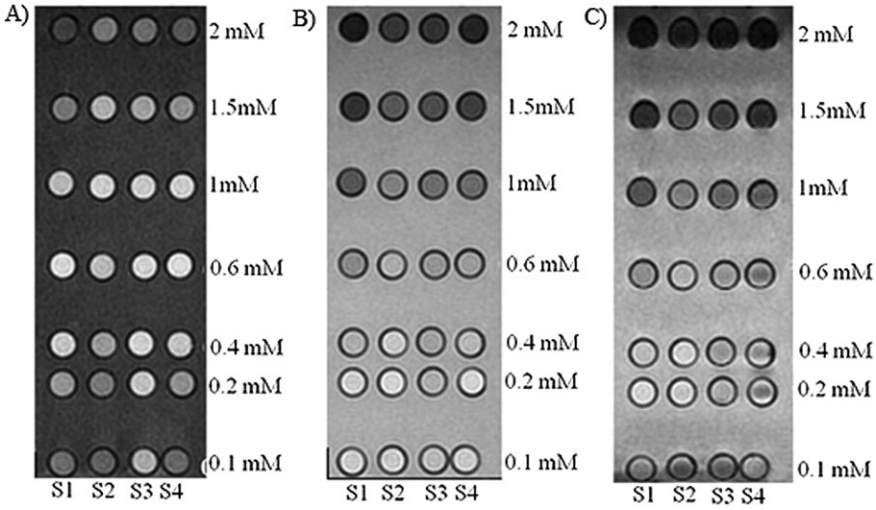

Figure 6. MR images of SPION samples in vials, A) T_1 (TR = 500 ms) and (TE = 11 ms). B) T2 (TR = 4000 ms) and (TE = 12 ms). C) T_2^* (TR = 300 ms) and (TE = 12 ms) for different concentrations of samples. S1: magnetite. S2: Herceptin targeted magnetoliposome. S3: Nanobody targeted magnetoliposome. S4: non targeted magnetoliposome. *In vitro* study was performed by 1.5 T GE MR Scanner at 25 °C with a 90 mm × 90 mm field of view (FOV), one acquisition, matrix size of 256 × 196 pixels and 5 mm slice thickness.

after 4 h (Fig. 4A) and PrestoBlue® viability assay (Fig. 4B) after 24 h for all types of nanoparticles are assessed separately for further confirmation. As anticipated, there is no significant cytotoxicity among samples during incubation times. Looking upon cell permeability or LDH assay, it was observed that all types of samples have no significant effects on cell membrane stability and permeability. The results indicating that in the actual conditions the iron oxide cores themselves did not play a crucial role but that the effects were solely due to the lipid bilayer. Therefore the inert magnetoliposomes are good candidate as contrast agents in clinical radiology and biomedical research today with minimal cytotoxicity and incompatibility effects.

3.4. Preparation of VHH-modified nanoparticles

Magnetoliposomes were obtained using the classical film method in a rotary evaporator under reduced pressure. The surface of the particles is PEGylated and activated by PEG_{2000}-DSPE and malemide-PEG_{2000}-DSPE respectively. The PEG chains introduced on the particle surface are responsible for the so-called 'stealth effect', preventing non-specific cell binding as well as adsorption of plasma proteins, in addition, provides a reactive malemide group which can be used for covalent binding of thiolated VHH by thioether bond formation (29,30). The SEC analysis of the supernatants revealed, that the VHH was quantitatively bound to the nanoparticle surface by effective percent near to 70% (Fig. 1). Therefore, the amounts of introduced sulfhydryl groups were optimized to achieve the highest efficiency in VHH conjugation to the particle surface. Since almost one free sulfhydryl group (per VHH molecule) was introduced, the number of adsorptive VHH binding to the particle surface could be roughly anticipated. Within our study it was observed, that increasing the conjugation time and temperature caused a slight problems in cell attachment and uptake. Likewise, the magnetoliposome's stability was decreased and some precipitation was appeared. Moreover, after a reaction time of 24 h multimeric conjugates have occurred. Thus, an average 27 μg VHH were attached per mg nanoparticle which corresponds to 58 VHH molecules per nanoparticles.

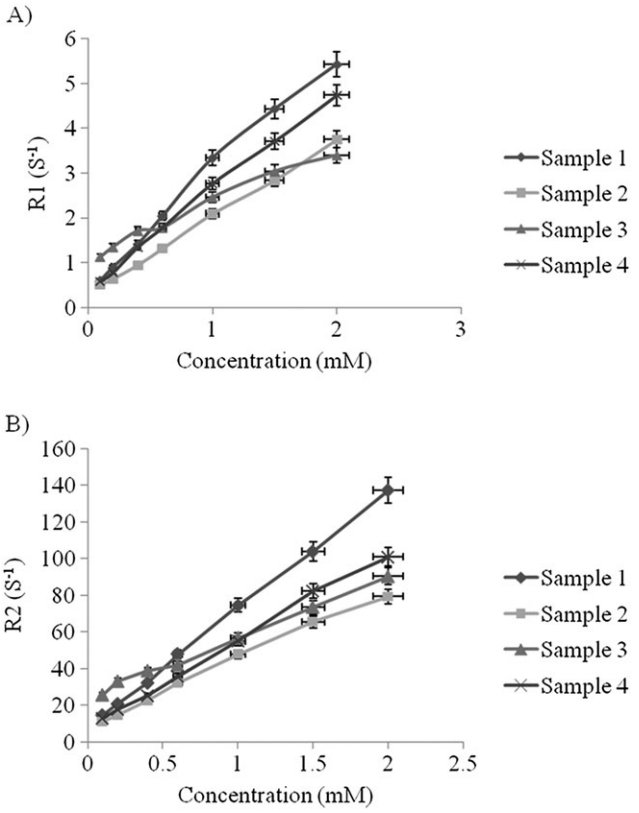

Figure 7. A) Longitudinal, R1 relaxation rates versus concentration for sample 1 to sample 4 respectively. B) Transverse, R2 relaxation rates versus concentration for sample 1 to 4 respectively.

Table 4. Transverse, Longitudinal relaxation times and r2/r1 ratios for the magnetite, nanobody targeted ML, Herceptin targeted ML and non-targeted ML

	r_2 (mM^{-1} s^{-1})	SD	r_1 (mM^{-1} s^{-1})	SD	$r_{2/}$ r_1
Sample 1 (magnetite)	64.63	0.75	2.59	0.10	24.92
Sample 2 (HER2-ML)	36.72	1.23	1.72	0.03	21.41
Sample 3 (Nb-ML)	32.90	0.98	1.21	0.07	27.28
Sample 4 (ML)	47.64	1.05	2.20	0.05	21.67

3.5. Storage stability of anti-HER2 VHH targeted magnetoliposomes

Storage stability of anti-HER2 VHH modified nanoparticles for the stability investigations, released anti-HER2 VHH was determined over a storage period of 4 weeks. Over the total storage time no anti-HER2 VHH was detectable in the supernatant. Likewise, the physicochemical properties _size and zetapotential_ did not change significantly (Fig. 5). Thus, targeted magnetoliposomes have long-term stability in biological solutions, such as buffer or aqueous phases, for at least one month. In some cases non covalent nanoparticles targeting show problems with colloidal storage stability. Therefore, in order to simplify the nanoparticle system we established a direct covalent linkage of anti-HER2 VHH. In a first step anti-HER2 VHH was thiolated and afterwards the thiolated VHH was coupled on the surface of the nanoparticles. Storage stability of the system over 4 weeks was demonstrated. This stability is required for using the system in cell culture and in vivo assays.

3.6. Magnetic properties of targeted and non-targeted MLs

According to T1, T2 and T2* weighted images with multiple TR and TE (Fig. 6), different signal intensities could be seen in a concentration dependent manner. So, different T1 and T2 relaxation times have been achieved as a result of different concentrations. The R1 and R2 map images were measured as shown in Fig. 7 (A), (B), and Table 4. The r2/r1 ratio was more than 2 for all USPION embedded specimens. The high r2/r1 as well as high r2 is the best combination of a negative contrast agent or T2 contrast agent, as it is obtained for pure magnetite (sample 1). These facts mean that the lipid composition of liposomes influences the relaxivity produced by the contrast agents encapsulated or incorporated within them. The engineering of nanoparticles with high relaxivity (and therefore contrast) is thus highly advantageous for specific targeting of receptors or antigens. Furthermore, the conjugation of biomolecules such as antibodies (average diameter ~10 nm) to the surface of nanoparticles for specific targeting may have an effect on the R2 characteristics due to the increase of overall apparent thickness of the coating. Depending on the effect of these biomolecules on surrounding water and its diffusion around the particle, such attachments may result in a decrease in the r2 relaxivity of the contrast agent. The amount of r2/r1 for all other samples including HER2 targeted magnetoliposome (sample 2), VHH targeted magnetoliposome (sample 3) and non-targeted magnetoliposome (sample 4) were between ~21 to ~28, which show the Magnetite embedded samples have enough negative contrast to be detectable by MR Imaging. Sample 3 shows the highest r2/r1 value, although it suffer the lowest r1 value. The near r2/r1 values for samples 4 and 2 show that the anti HER2 loading process was not affected the amount of magnetite content of non-targeted magnetoliposome. As indicated, the encapsulation of a hydrophilic Fe-based contrast agent in liposomes results in reduction of the relaxivity. Because of their ability to provide tumor targeted imaging, anti-HER2 MLs represent a potentially powerful strategy for the diagnostics and treatments of HER2-overexpressing cancers. These nanocarriers bind to and internalize in target cells but are non-reactive with normal cells.

4. CONCLUSION

In the present work, we have developed a set of physico-chemical protocols to prepare magnetic nanoparticles that possess accurate sizes, shapes, compositions, relaxivities, stability and surface charges. These features, in turn, can be harnessed to adjust the toxicity and stability of the nanoparticles and, further, to load functionalities, via various mechanisms, onto the nanoparticle surfaces. These capabilities have greatly expanded the role of magnetic nanoparticles, enabling real-time targeting, imaging, and therapy. Classical MLs targeted by anti-Her2 VHH and Herceptin, were used as a model system for analysis the effect of surface decorating on relaxometry. It was shown that inert and PEGylated MLs and also free USPIONs are biocompatible with minimum severe effects on cell plasma membrane. Previous studies also confirmed that MLs toxicity depends on the nature of the lipid, the size and physico-chemical characteristics of the liposome formulations (28). The need to assess the effect of targeting on the properties of nano particles caused we analyzed anti-Her2 VHH and Herceptin conjugated MLs as contrast agents in MRI. The high ratio r2/r1 as well as high r2 in targeted MLs are the best combination of a negative contrast agent as it is obtained for pure magnetite. While the outlook is clear and exciting, it is fair to admit that we are at a relatively early stage of development. In fact, there is a complex interplay between coating thickness, coating chemistry, and overall MR contrast generated; all these need to be carefully examined for the optimization of USPIONs-based contrast agents. *In vitro* and *in vivo* assay are necessary and unavoidable that are being undertaken in our laboratories.

Acknowledgements

This paper was supported by Faculty of Medical Sciences, Tarbiat Modares University, Tehran, Iran and School of Allied Medical Sciences, Iran University of Medical Sciences, Tehran, Iran reference 16550.

REFERENCES

1. Bonnet CS, Tóth É. MRI contrast agents. In Ligand Design in Medicinal Inorganic Chemistry, Storr T (ed). John Wiley & Sons, Ltd: Chichester, UK, 2014; 321–354.
2. Martina M-S, Fortin J-P, Ménager C, Clément O, Barratt G, Grabielle-Madelmont C, Gazeau F, Cabuil V, Lesieur S. Generation of superparamagnetic liposomes revealed as highly efficient MRI contrast agents for *in vivo* imaging. J Am Chem Soc 2005; 127(30): 10676–10685.
3. Faria M, Cruz M, Gonçalves M, Carvalho A, Feio G, Martins M. Synthesis and characterization of magnetoliposomes for MRI contrast enhancement. Int J Pharm 2013; 446(1): 183–190.
4. Estelrich J, Sánchez-Martín MJ, Busquets MA. Nanoparticles in magnetic resonance imaging: from simple to dual contrast agents. Int J Nanomedicine 2015; 10: 1727.

5. Paul KG, Frigo TB, Groman JY, Groman EV. Synthesis of ultrasmall superparamagnetic iron oxides using reduced polysaccharides. Bioconjug Chem 2004; 15(2): 394–401.
6. Chen S. Polymer-coated iron oxide nanoparticles for medical imaging: Massachusetts Institute of Technology; 2010.
7. Soenen SJ, Velde GV, Ketkar-Atre A, Himmelreich U, De Cuyper M. Magnetoliposomes as magnetic resonance imaging contrast agents. Wiley Interdiscip Rev Nanomed Nanobiotechnol 2011; 3(2): 197–211.
8. Chen Y, Tao J, Xiong F, Zhu J, Gu N, Geng K. Characterization and *in vitro* cellular uptake of PEG coated iron oxide nanoparticles as MRI contrast agent. Pharmazie 2010; 65(7): 481–486.
9. Frascione D, Diwoky C, Almer G, Opriessnig P, Vonach C, Gradauer K, Leitinger G, Mangge H, Stollberger R, Prassl R. Ultrasmall superparamagnetic iron oxide (USPIO)-based liposomes as magnetic resonance imaging probes. Int J Nanomedicine 2012; 7: 2349.
10. Immordino ML, Dosio F, Cattel L. Stealth liposomes: review of the basic science, rationale, and clinical applications, existing and potential. Int J Nanomedicine 2006; 1(3): 297.
11. Li J, Sharkey CC, Huang D, King MR. Nanobiotechnology for the therapeutic targeting of cancer cells in blood. Cell Mol Bioeng 2015; 8(1): 137–150.
12. Dawidczyk CM, Russell LM, Searson PC. Nanomedicines for cancer therapy: state-of-the-art and limitations to pre-clinical studies that hinder future developments. Front Chem 2014; 2.
13. Dilnawaz F, Singh A, Mohanty C, Sahoo SK. Dual drug loaded superparamagnetic iron oxide nanoparticles for targeted cancer therapy. Biomaterials 2010; 31(13): 3694–3706.
14. Kievit FM, Stephen ZR, Veiseh O, Arami H, Wang T, Lai VP, Park JO, Ellenbogen RJ, Disis ML, Zhang M. Targeting of primary breast cancers and metastases in a transgenic mouse model using rationally designed multifunctional SPIONs. ACS Nano 2012; 6(3): 2591–2601.
15. Pourtau L, Oliveira H, Thevenot J, Wan Y, Brisson AR, Sandre O, Miraux S, Thiaudiere E, Lecommandoux S. Antibody-functionalized magnetic polymersomes: *in vivo* targeting and imaging of bone metastases using high resolution MRI. Adv Healthc Mater 2013; 2(11): 1420–1424.
16. Bulte JW, de Cuyper M, Despres D, Frank JA. Preparation, relaxometry, and biokinetics of PEGylated magnetoliposomes as MR contrast agent. J Magn Magn Mater 1999; 194(1): 204–209.
17. Yuan Y, Rende D, Altan CL, Bucak S, Ozisik R, Borca-Tasciuc D-A. Effect of surface modification on magnetization of iron oxide nanoparticle colloids. Langmuir 2012; 28(36): 13051–13059.
18. Garbuzenko O, Barenholz Y, Priev A. Effect of grafted PEG on liposome size and on compressibility and packing of lipid bilayer. Chem Phys Lipids 2005; 135(2): 117–129.
19. Vestal CR, Zhang ZJ. Effects of surface coordination chemistry on the magnetic properties of MnFe2O4 spinel ferrite nanoparticles. J Am Chem Soc 2003; 125(32): 9828–9833.
20. LaConte LE, Nitin N, Zurkiya O, Caruntu D, O'Connor CJ, Hu X, Bao G. Coating thickness of magnetic iron oxide nanoparticles affects R2 relaxivity. J Magn Reson Imaging 2007; 26(6): 1634–1641.
21. Jamnani FR, Rahbarizadeh F, Shokrgozar MA, Ahmadvand D, Mahboudi F, Sharifzadeh Z. Targeting high affinity and epitope-distinct oligoclonal nanobodies to HER2 over-expressing tumor cells. Exp Cell Res 2012; 318(10): 1112–1124.
22. Oghabian MA, Gharehaghaji N, Masoudi A, Shanehsazzadeh S, Ahmadi R, Majidi RF, Reza F, Hosseini H. Effect of coating materials on lymph nodes detection using magnetite nanoparticles. Adv Sci Eng Med 2013; 5(1): 37–45.
23. Sabaté R, Barnadas-Rodríguez R, Callejas-Fernández J, Hidalgo-Álvarez R, Estelrich J. Preparation and characterization of extruded magnetoliposomes. Int J Pharm 2008; 347(1): 156–162.
24. Wray W, Boulikas T, Wray VP, Hancock R. Silver staining of proteins in polyacrylamide gels. Anal Biochem 1981; 118(1): 197–203.
25. García-Jimeno S, Escribano E, Queralt J, Estelrich J. Magnetoliposomes prepared by reverse-phase followed by sequential extrusion: characterization and possibilities in the treatment of inflammation. Int J Pharm 2011; 405(1): 181–187.
26. Soenen SJ, De Cuyper M, De Smedt SC, Braeckmans K. Investigating the toxic effects of iron oxide nanoparticles. Methods Enzymol 2012; 509: 195–224.
27. Soenen SJ, Himmelreich U, Nuytten N, De Cuyper M. Cytotoxic effects of iron oxide nanoparticles and implications for safety in cell labelling. Biomaterials 2011; 32(1): 195–205.
28. Soenen SJ, Brisson AR, De Cuyper M. Addressing the problem of cationic lipid-mediated toxicity: the magnetoliposome model. Biomaterials 2009; 30(22): 3691–3701.
29. Lin W, Garnett MC, Schacht E, Davis SS, Illum L. Preparation and *in vitro* characterization of HSA-mPEG nanoparticles. Int J Pharm 1999; 189(2): 161–170.
30. Steinhauser I, Spänkuch B, Strebhardt K, Langer K. Trastuzumab-modified nanoparticles: optimisation of preparation and uptake in cancer cells. Biomaterials 2006; 27(28): 4975–4983.

